

**Hydrodynamic behavior near dynamical criticality of a facilitated conservative lattice gas**Clément Erignoux <sup>\*</sup>*Inria DRACULA, ICJ UMR5208, CNRS, Ecole Centrale de Lyon, INSA Lyon, Université Claude Bernard Lyon 1, Université Jean Monnet, 69603 Villeurbanne, France*Alexandre Roget <sup>†</sup>*Inria PARADYSE, LPP UMR8524, Université de Lille, 59655 Villeneuve-d'Ascq, France*Assaf Shapira <sup>‡</sup>*Université Paris Cité, CNRS, UMR 8145, MAP5, Campus Saint-Germain-des-Prés, 75006 Paris, France*Marielle Simon <sup>§</sup>*Université Claude Bernard Lyon 1, ICJ UMR5208, CNRS, Ecole Centrale de Lyon, INSA Lyon, Université Jean Monnet, 69622 Villeurbanne, France and GSSI, Viale Francesco Crispi 7, 67100 L'Aquila, Italy*

(Received 18 March 2024; accepted 1 August 2024; published 3 September 2024)

We investigate a  $2d$ -conservative lattice gas exhibiting a dynamical active-absorbing phase transition with critical density  $\rho_c$ . We derive the hydrodynamic equation for this model, showing that all critical exponents governing the large scale behavior near criticality can be obtained from two independent ones. We show that as the supercritical density approaches criticality, distinct length scales naturally appear. Remarkably, this behavior is different from the subcritical one. Numerical simulations support the critical relations and the scale separation.

DOI: [10.1103/PhysRevE.110.L032101](https://doi.org/10.1103/PhysRevE.110.L032101)

*Introduction.* Models displaying dynamical phase transitions have attracted increasing scrutiny in recent years. Such models are tightly related to “self-organized criticality,” and may also illustrate how hyperuniform structures [1] emerge in nature [2,3]. Their complexity prevents from building a universal framework, and this is why some paradigmatic models are currently under deep mathematical and physical investigation (as for instance sandpiles [4], or random organization models [5]). Open systems dynamically adjust their density in order to reach a critical state at density  $\rho_c$ , often displaying nontrivial scaling properties. This phenomenon manifests itself, in a closed system, as a dynamical phase transition: below  $\rho_c$ , the system reaches an absorbing state, while above  $\rho_c$ , it remains in a quasistationary active state.

A fundamental example of such a model is the constrained conservative lattice gas (CLG) [6], also referred to as facilitated exclusion process in the recent literature. It is defined as an exclusion particle system (i.e., any system site cannot contain more than one particle) on a  $d$ -dimensional lattice, where so-called active particles jump randomly at rate one to each empty nearest neighbor [7]. As represented in Fig. 1, a particle is considered active if at least one of its neighboring sites is also occupied, and the total number of particles is conserved. Related models featuring an absorbing phase transition have

generated an intense research activity, like for instance the paradigm Manna sandpile model [8–11]. In particular, many of these models, including the CLG, exhibit a hyperuniform critical state [12,13], for which we still have a limited knowledge. The CLG has been investigated numerically in [6,12–14] when  $d \geq 2$ , and theoretically in [15–21] when  $d = 1$ . We focus here on the two-dimensional case, and recall some previous results already obtained in the one-dimensional case. While we expect to see the same general picture in higher dimensions, numerical studies of the model become more complicated. Some critical exponents in  $d = 3$  are found in [12], and we expect the critical relations laid out in this paper to hold (though we do not provide verification).

Clearly, this system remains active whenever  $\rho > 1/2$ , and could reach an absorbing state whenever  $\rho \leq 1/2$ . It appears, however, that in dimension  $d \geq 2$ , the dynamical critical density  $\rho_c$  is strictly smaller than  $1/2$ . That is, in the regime  $(\rho_c, 1/2]$ , even though an absorbing state will be ultimately reached in any finite system, on physically relevant timescales a quasistationary active state is observed. In order to illustrate this phenomenon, the average absorption time is numerically represented in Fig. 2 in both subcritical and supercritical regimes.

The CLG is reflection symmetric and isotropic, and therefore its macroscopic density profile  $\rho$ , taken in the diffusive space-time scaling limit, is expected to be a solution to the parabolic equation  $\partial_t \rho = \text{div}(D(\rho)\nabla\rho)$  with scalar diffusion coefficient  $D(\rho)$ . In the subcritical regime  $\rho < \rho_c$  the particles become blocked in subdiffusive time scales [see Fig. 2(a)], therefore,  $D(\rho) = 0$ . When the initial profile has

<sup>\*</sup>Contact author: [clement.erignoux@inria.fr](mailto:clement.erignoux@inria.fr)<sup>†</sup>Contact author: [alexandre.roget@inria.fr](mailto:alexandre.roget@inria.fr)<sup>‡</sup>Contact author: [assaf.shapira@normalesup.org](mailto:assaf.shapira@normalesup.org)<sup>§</sup>Contact author: [msimon@math.univ-lyon1.fr](mailto:msimon@math.univ-lyon1.fr)

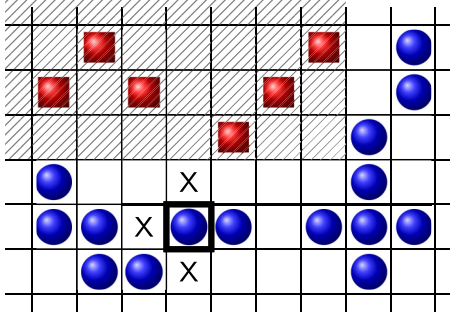


FIG. 1. Blue circle particles are active, red square particles are frozen. As an example, the active particle highlighted with  $\square$  can jump to one of its three neighbors indicated with X. The dashed region corresponds to the frozen phase.

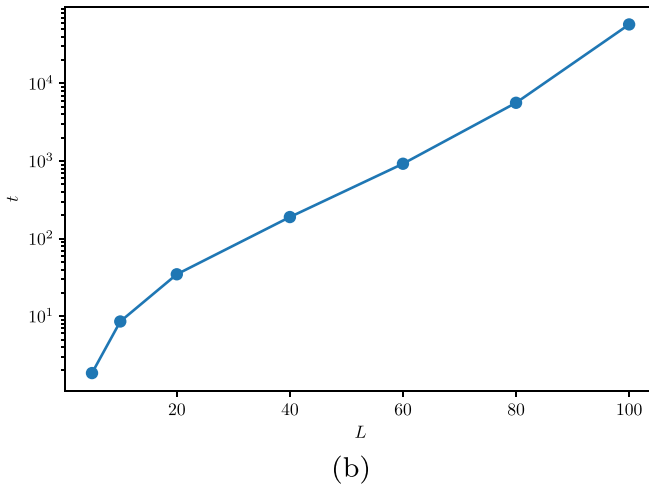
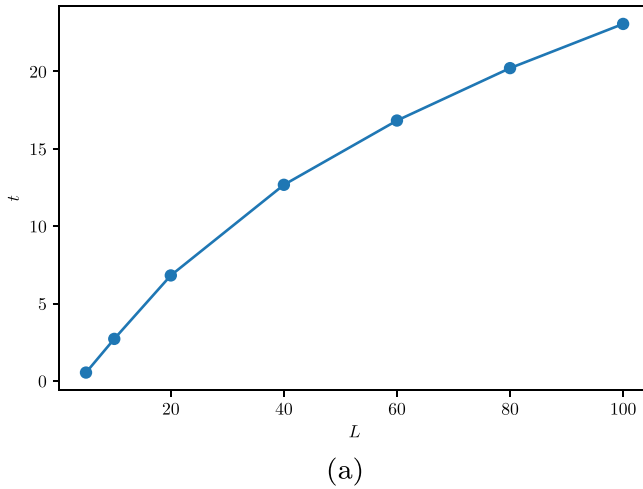


FIG. 2. Median absorption time in a closed box, of size changing from 5 to 100. In the subcritical phase (a),  $\rho = 0.279$ , the absorption time grows sublinearly with the system size. In the supercritical phase (b),  $\rho = 0.334$ , it grows exponentially fast at large  $L$ . In fact, the figure illustrates nicely that at  $\rho = 0.334$  the geometric correlation length, which separates the absorbing regime from the quasistationary regime, is roughly  $\xi \approx 20$ , which is the approximate point where the exponential growth begins.

both subcritical and supercritical regions, the supercritical phase progressively invades the subcritical “frozen” areas. That is, one should interpret the above hydrodynamic equation as a Stefan problem. In dimension one this result is established mathematically in [19], and exploits the explicit expression of the stationary states, a feature that is lost in higher dimensions.

In this Letter we explore the scaling properties of the two-dimensional model, with a particular focus on the active phase. We study the critical exponents for all relevant macroscopic quantities, both theoretically and numerically, as it has been done for other models, for instance in [22]. We are able to deduce relationships between those critical exponents, which are of independent interest, and check them by simulations.

*Macroscopic observables.* Of particular interest are the critical and near criticality behavior of the model. It has been noted in [12] that the CLG could have two separate length scales near criticality. While in their simulations these two scales seem to coincide, we will see here that in the supercritical phase they differ. Let us define the following.

(i) The geometric correlation length  $\xi_{\perp}$ : this is the scale which is mostly used in the literature [[23], Sec. 3.3], and is the one discussed in [6]. It describes the spread of activity. More precisely, to sustain activity, particle clusters must self-activate, i.e., a particle activates its neighbor, which further activates its neighbors, until closing a cycle and reactivating the particle we started with. The diameter of this self-activated structure is described by the geometric correlation length  $\xi_{\perp}$ .

This means that, for a finite system of size  $L$ , if  $L \ll \xi_{\perp}$ , then there is no quasistationary state, and in that case, activity will decay until dying out. On the other hand, if  $L \gg \xi_{\perp}$ , then the activity behaves in the same manner as  $L = \infty$ .

(ii) The two-point correlation length  $\xi_{\times}(\rho)$ : This is the length over which the two-point correlation function decays. This scale is referred to as the crossover length in [12], where the authors show, in the subcritical phase, that below  $\xi_{\times}$  the absorbing state is hyperuniform [1,24]; above  $\xi_{\times}$  it is Poissonlike.

Both length scales diverge when approaching criticality, as  $\xi_{\perp} \sim (\rho - \rho_c)^{-\nu_{\perp}}$  and  $\xi_{\times} \sim (\rho - \rho_c)^{-\nu_{\times}}$ , for some critical exponents  $\nu_{\perp}$  and  $\nu_{\times}$ , which we now investigate.

In [6,12], several other critical exponents are determined. Notably, in the latter the authors show that the CLG’s absorbing state is hyperuniform, i.e. the number of particles  $N$  in a ball or radius  $R$  has standard deviations of order  $R^{\zeta}$ , for  $\zeta$  smaller than  $d/2$ .

We are interested in the hydrodynamic behavior of the CLG, whose diffusion coefficient  $D(\rho)$  behaves, close to  $\rho_c$ , as  $(\rho - \rho_c)^{\alpha}$  for some exponent  $\alpha$ . In order to understand the noise’s amplitude, we also consider the compressibility  $\chi(\rho) \sim (\rho - \rho_c)^{\gamma}$ , defined as the sum of the two-point correlation function over the infinite lattice. For the CLG, the dominant parameter for the system is the density of active particles,  $\rho_a(\rho)$ . However, the notion of active particles is in fact ambiguous, since one may or may not count as active particles who are fully surrounded by other particles (and therefore cannot move). For this reason, we distinguish between  $\rho_a(\rho) \sim (\rho - \rho_c)^{\beta}$ , the density of particles having at least one occupied neighbor (which is the one considered in [6]), and the activity  $a(\rho) \sim (\rho - \rho_c)^b \leq 3\rho_a$ , which counts

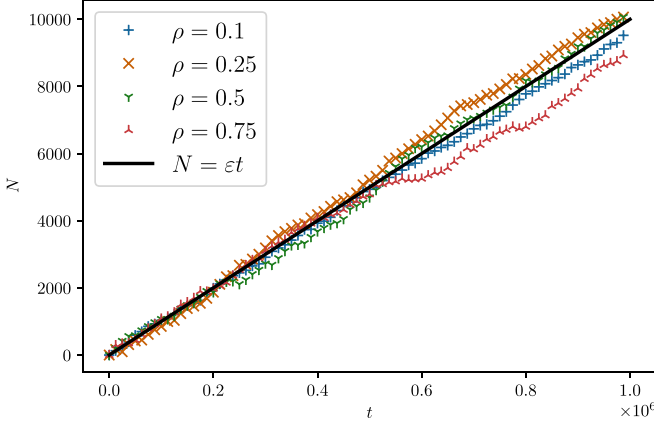


FIG. 3.  $N_t$  as a function of  $t$  for different reservoir densities. See Eq. (13).

the local number of possible jumps. We will see further that in fact both exponents  $\beta$  and  $b$  coincide (Fig. 4). This means that the perimeter of clusters of active particles is of the same order as their volume.

*Relations between critical exponents.* By numerical simulations we are able to get all the critical exponents in the case  $d = 2$ . In dimension  $d = 1$ , we have exact values, as discussed below.

A number of relations can be derived between the relevant critical exponents [23]. Most of them are standard, a detailed derivation will be given in a companion article [25]. The first one ties the compressibility to the particle fluctuations and the activity correlation length, as

$$\gamma = v_{\times}(d - 2\zeta). \quad (1)$$

This relation can be obtained by considering the structure factor  $S_{\rho}(k)$  (see [[26], Sec. II.2.1]), which encapsulates the two-point statistics of the distribution at a fixed time [24]. By the scaling hypothesis,  $S_{\rho}(k)$  can only depend on  $k$  via the combination  $\xi_{\times}k$ . Moreover,  $S_{\rho}(0) = \chi(\rho)$ , and at criticality  $S_{\rho_c}(k) \sim C|k|^{d-2\zeta}$  when  $|k|$  is small. These three facts impose the form

$$S_{\rho}(k) = \chi \left( 1 + \frac{C}{\chi \xi_{\times}^{d-2\zeta}} |\xi_{\times}k|^{d-2\zeta} \right), \quad (2)$$

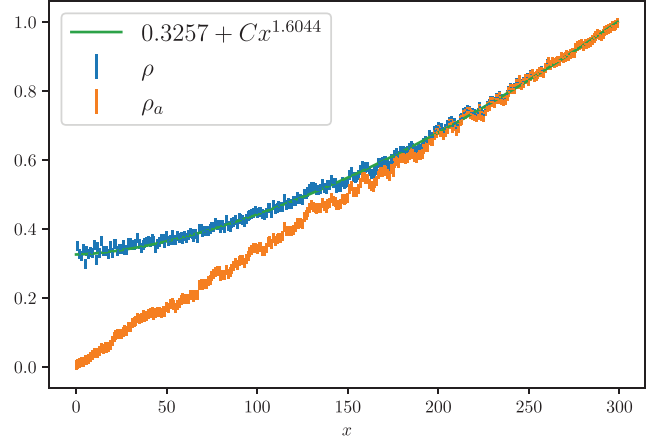
and hence  $\chi \xi_{\times}^{d-2\zeta}$  remains of order one as  $\rho \rightarrow \rho_c$ . This implies Eq. (1).

A similar scaling relation can be obtained for the geometric correlation length. Indeed, at scales smaller than  $\xi_{\perp}$  the system looks critical, so that the critical density fluctuations are larger than  $\rho - \rho_c$ , and “hide” the off criticality. The scale  $\xi_{\perp}$  is therefore characterized by the relation  $\xi_{\perp}^{\zeta-d} \approx \rho - \rho_c$ . This yields the following relation:

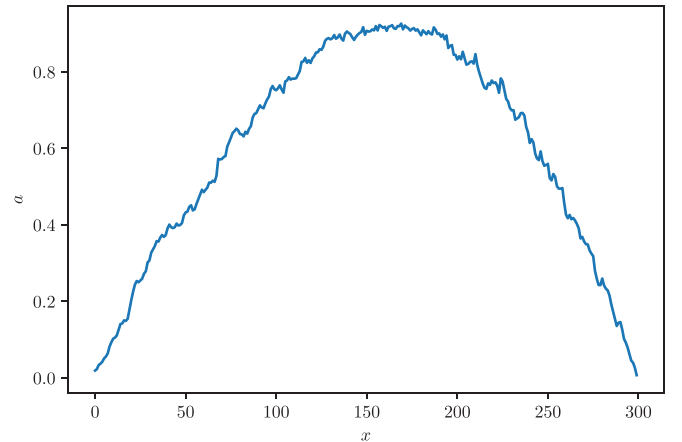
$$v_{\perp}(d - \zeta) = 1. \quad (3)$$

The next relation stems from Einstein’s relation  $D = \sigma/\chi$  (see [[26], (2.72), Sec. II.2.5]) and the fact that the noise amplitude is determined by the number of possible particle jumps  $\sigma = a$  (see [[26], Sec. II.2] for instance); this leads to

$$\alpha = b - \gamma. \quad (4)$$



(a)



(b)

FIG. 4. Simulating  $\rho(x)$ ,  $\rho_a(x)$ , and  $a(x)$  in a system with reservoirs  $\lambda_l = 0$ ,  $\lambda_r = 1$ . On the top we see as expected that  $\rho_a$  (the bottom curve) is linear in  $x$ . We also observe the the fitted curve  $0.3257 + Cx^{1.6004}$  is almost exactly covered by the measured values of  $\rho$ .

Finally, the following relation is a consequence of a particular property of the CLG, called gradient condition [26,27], which relies on well-chosen jump rates for the system. Under this condition,

$$\partial_t \langle n_i \rangle = \sum_{j \sim i} \{ \langle n_{a,j} \rangle - \langle n_{a,i} \rangle \}, \quad (5)$$

where  $\langle n_i \rangle$  (resp.  $\langle n_{a,i} \rangle$ ) denotes the average number of particles (resp. active particles) at site  $i$ . At the macroscopic level, this identity translates as

$$\partial_t \rho = \Delta(\rho_a(\rho)), \quad (6)$$

and yields in turn that  $D(\rho) = \rho'_a(\rho)$ . Near criticality, this implies

$$\alpha = \beta - 1. \quad (7)$$

Note that Eqs. (4) and (7) give  $\beta - b = 1 - \gamma$ . As an interesting consequence, the fact that  $\beta = b$ , i.e.. that clusters of active particles have volume and perimeter of the same order, implies  $\gamma = 1$ . In Table I we give all exponents in both  $d = 1$

TABLE I. Critical exponents related to observables, in  $d = 1$  and  $d = 2$ . The one-dimensional exponents are exact, see below. In the two-dimensional case, the first line is obtained either directly from our simulation results, or extracted from scaling relations. The second line contains simulation results taken from previous articles. In our case, the exponents  $\beta$  and  $b$  are taken from the simulation of Fig. 4(a). The exponent  $\gamma$  is simulated twice: the value 1 is obtained from Fig. 4 and Eq. (4); the value 1.07 is obtained from Fig. 5. The exponent  $\nu_\times$  is extracted from the simulation of Fig. 5 and then  $\zeta$  is computed using (1) with  $\gamma = 1$ . The exponent  $\alpha$  is calculated using Eq. (7),  $\nu_\perp$  from Eq. (3), and  $z$  from (11).

obs.	$D$	$\chi$	$\xi_\perp$	$\xi_\times$	$\text{Var}(N)$	$\rho_a$	$a$	
exp.	$\alpha$	$\gamma$	$\nu_\perp$	$\nu_\times$	$\zeta$	$\beta$	$b$	$z$
$d = 1$	0	1	1	1	0	1	1	2
$d = 2$	-0.38	1 and 1.07	0.77	1.8	0.72	0.62	0.62	1.51
			0.78 <sup>a</sup>		0.775 <sup>b</sup>	0.63 <sup>a</sup>		1.52 <sup>a</sup>

<sup>a</sup>Obtained in [6]

<sup>b</sup>Obtained in [12]

and  $d = 2$  cases. The former are exact values, while the latter are numerically computed.

*Hydrodynamics and scale invariance.* Near criticality, we are interested in the macroscopic evolution of  $u := \rho - \rho_c$ . It evolves according to the fluctuating hydrodynamic equation (e.g., [[26], II.2.9])

$$\partial_t u = \text{div}(D\nabla u + \sqrt{2D\chi}W). \quad (8)$$

The noise  $W$  depends on the scale at which we look: at distances above  $\xi_\times$ , correlations are small and  $W$  is white noise, while for distances smaller than  $\xi_\times$  the noise  $W$  will have nontrivial correlations

$$\langle W(0,0) \cdot W(x,t) \rangle = \begin{cases} \delta(t)\delta(x), & |x| > \xi_\times, \\ \delta(t)|x|^{-\vartheta}, & |x| < \xi_\times, \end{cases} \quad (9)$$

for some exponent  $\vartheta$ . In the regime below  $\xi_\times$ , the density fluctuations are proportional to  $\ell^{\zeta-d}$ , hence Eq. (8) must be invariant under the parameter rescaling

$$(u, x, t) \mapsto \left( \frac{u}{\ell^{d-\zeta}}, \frac{x}{\ell}, \frac{t}{\ell^z} \right). \quad (10)$$

This forces  $\vartheta$  to be equal  $1 - \zeta/d$ , and

$$z = (\zeta - d)(1 - \beta) + 2. \quad (11)$$

We emphasize that on a length above  $\xi_\times$  the scale invariance is not the same, and in particular the dynamic exponent  $z$  will change (see [25]). This scale separation has been noted qualitatively in [6].

*One-dimensional case.* The one-dimensional case  $d = 1$  has been recently under scrutiny, and its macroscopic evolution is now quite well understood. It has been proved rigorously [18,19] that the critical density is given by  $\rho_c = 1/2$ , and the diffusive supercritical phase progressively invades the subcritical phase via flat interfaces, until either one of the phases disappears. In this respect, a crucial feature of the one-dimensional case lies in its explicit supercritical grand canonical states  $\pi_\rho$  either parametrized by the density  $\rho \geq 1/2$  or the active density  $\rho_a(\rho) = (2\rho - 1)/\rho$ . These

grand canonical states can be defined sequentially, by filling an arbitrary site with probability  $\rho$ , and then following each empty site by a particle with probability one, but each particle by another particle with probability  $\rho_a(\rho)$ .

Precisely, the hydrodynamic limit in  $d = 1$  is given by  $\partial_t \rho = \partial_x(D(\rho)\partial_x \rho)$ , with diffusion coefficient

$$D(\rho) = \rho'_a(\rho) = \rho^{-2} \mathbf{1}_{\{\rho > \rho_c\}} \quad (12)$$

and critical exponent  $\alpha = 0$ . The explicit construction of the grand-canonical state  $\pi_\rho$  yields the other observables for  $\rho \geq \rho_c$ , as well as their critical exponent (see [20]): namely the activity  $a(\rho) = \rho^{-1}(1 - \rho)(2\rho - 1)$  with  $b = 1$ , and the compressibility  $\chi(\rho) = \rho(1 - \rho)(2\rho - 1)$ , with  $\gamma = 1$ . Moreover, the stationary measure can be seen as a nearest-neighbor spin system with chemical potential  $\mu$ , and an interaction which gives infinite costs to two neighboring empty sites. This can be solved using standard methods involving the transfer matrix (see [[28], Chapter 6]), which here is given by

$$\begin{pmatrix} 0 & e^{-\mu} \\ 1 & e^{-\mu} \end{pmatrix}.$$

All the relevant quantities and exponents for the one-dimensional model are listed in Table I.

*Numerical simulations.* We note that in finite systems the critical density depends slightly on the geometry, so that in the analysis of the simulated data we do not enforce a single critical density for systems of different sizes or boundary conditions. Rather, we leave  $\rho_c$  as a parameter for the regression. Since  $L$  equals 300 in one simulation and 100 in the other, it is not surprising that we obtain values of  $\rho_c$  who differ by  $\mathcal{O}(1/L)$ .

In order to numerically derive the diffusion coefficient and verify relation (7), we simulate a cylindrical system, i.e., periodic in the vertical direction, of size  $L$  put in contact at the left and right boundaries with particle reservoirs with respective densities  $\lambda_l$  and  $\lambda_r$ . More specifically, at the boundary, particles are removed at rate  $1 - \lambda_l$ ,  $1 - \lambda_r$ , and empty sites are filled at rate  $\lambda_l$ ,  $\lambda_r$ . In our simulations, boundary particles are always considered active.

When  $\lambda_l = \lambda_r = \lambda$ , the system reaches a quasistationary state with density  $\rho(\lambda)$ . For our particular choice of boundary interactions,  $\rho_a(\rho(\lambda)) = \lambda$ , meaning that the reservoirs enforce the density of active particles and not the total density of particles. This relation is, however, not universal, and depends on the exact boundary dynamics considered.

In order to estimate the diffusion coefficient, we fix  $\lambda_l = \lambda$  and  $\lambda_r = \lambda + \varepsilon$  with small  $\varepsilon > 0$ . We measure the total net number of particles  $N_t$  crossing the system up to time  $t$ . In general, we expect the current to be proportional to  $\varepsilon$ ,

$$\frac{N_t}{t} = K(\lambda)\varepsilon, \quad (13)$$

where  $K(\lambda) = D(\rho)\rho'(\lambda)$ . Since our system is gradient and for our specific choice of reservoirs, we should obtain  $K = 1$ , which is verified by our simulation, see Fig. 3. In particular, this shows that  $\alpha = \beta - 1$ .

In more general models (for instance when the gradient property is not satisfied) we do not necessarily expect  $K$  to

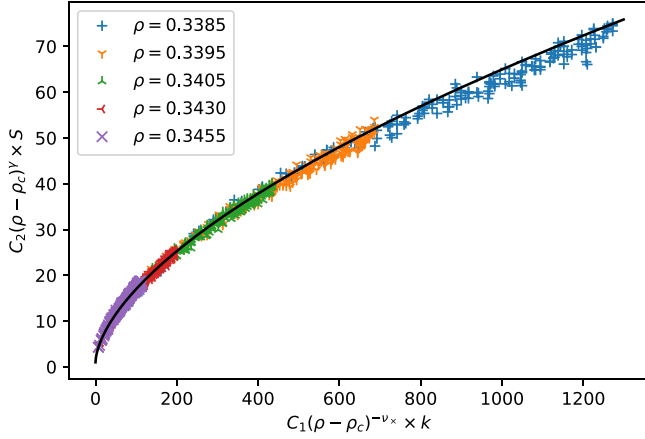


FIG. 5. We show here a collapse of  $S_\rho(k)$  for different values of  $\rho$ . The parameters  $C_1 = 0.03$ ,  $C_2 = 0.71$ ,  $\rho_c = 0.3361$ ,  $\nu_x = 1.77$ ,  $\gamma = 1.07$  are adjusted to best fit Eq. (2). That is, we find that  $\chi(\rho) = 0.61(\rho - 0.3361)^{-1.07}$  and  $\xi_x = 0.03(\rho - 0.3361)^{-1.77}$ . Indeed, after this rescaling the curves  $S_\rho(k)$  collapse as expressed in Eq. (2). The fit (black curve) is given by  $S_\rho(k) = 0.61(\rho - 0.3361)^{1.07} + 0.07|k|^{0.60}$ .

be constant, but still of order 1 (namely, neither diverging nor decaying as  $\rho \rightarrow \rho_c$ ).

The scaling exponents  $\beta$  and  $b$  can be found by simulating the system with cylindrical geometry, maintaining one reservoir at density  $\lambda_l = 0$  and the other one at density  $\lambda_r = 1$ . We then measure, at each section  $x$  of the cylinder,  $\rho(x)$ ,  $\rho_a(x)$ , and  $a(x)$ ; see Fig. 4.

Thanks to the gradient property of the model and our choice of reservoirs,  $\rho_a$  grows linearly with the horizontal distance, from  $\lambda_l$  at  $x = 0$  to  $\lambda_r$  at  $x = 1$ . This is verified in our simulation (Fig. 4(a)). Thanks to this result, the relation  $\rho_a \propto (\rho - \rho_c)^\beta$  can then be written as  $\rho \sim \rho_c + x^{1/\beta}$ . By fitting  $\rho(x)$  in Fig. 4(a) we obtain  $\beta = 1.60^{-1} = 0.62$ . Finally, noting that for small  $x$  the activity  $a$  is linear in  $x$  (Fig. 4(b)), we conclude  $\beta = b$ .

In order to find the remaining exponents, we estimate the structure factor  $S_\rho(k)$  for different values of  $\rho$ . This is done on a system with periodic boundaries (in both directions). By fitting the data to Eq. (2), posing  $\chi = C_\chi(\rho - \rho_c)^\gamma$  and  $\xi_x = C_x(\rho - \rho_c)^{-\nu_x}$ , we obtain the values in Table I; see Fig. 5.

All the simulations used in this article are open access, available in Ref. [29].

**Conclusion.** In this article, we discussed the critical scaling for the CLG. We saw that there are three independent critical exponents,  $\beta$ ,  $b$ , and  $\zeta$ , that all other exponents ( $\alpha$ ,  $\gamma$ ,  $\nu_\perp$ ,  $\nu_x$ ,  $z$ ) could be deduced from. Moreover, due to repulsion, active cluster sizes are of order one, so their perimeter is proportional to the volume, thus  $\beta = b$  and all scaling is described by two independent exponents. In fact, we expect the scaling relations stated here to hold in a much larger generality than the two-dimensional CLG, and that  $\gamma = 1$  should hold as well in repulsive 2D systems, see [22] for

similar relations and comparison to other models. Note that we have used the gradient condition in order to derive Eqs. (4) and (7). This condition is very sensitive to small changes in the dynamics, but we believe that scaling exponents and relations are universal, and depend much less on perturbations of the dynamics. At the same time, it is worth noting that some “highly nongradient” systems are known not to satisfy these relations (e.g., the Kob-Andersen model, in which  $\alpha = \infty$  [30,31]), but this phenomenon is due to the formation of very specific cooperative structures.

We numerically computed several critical exponents for the  $2d$ -CLG (see Table I), and confronted them both with those critical relations, and the numerical values in [6] and [12] for CLG with simultaneous jumps. We obtained very good agreement between them, with the exception of  $\zeta$  and  $\nu_x$ . While our numerical values fit the theoretical relations introduced above, they are different from those of [12]. The reason seems to be that we approach the critical state from  $\rho > \rho_c$ , while [12] do from  $\rho < \rho_c$ . Recently, [13,32] went further investigating the approach to hyperuniformity from the subcritical regime; on the contrary to [12], they find that the critical exponent  $\nu_x$  (which [13] denote  $\gamma_1$ ) is different from  $\nu_\perp$ . That is, a separation between two different length scales is also present in the subcritical regime, but with an exponent  $\nu_x$  different from the supercritical one.

We emphasize the existence of two distinct correlation lengths, one characterizing the size of self-activating clusters, and the other one characterizing the two-points correlation decay. This distinction is a specific feature of the quasistationary regime ( $\rho_c, 1/2$ ), and for this reason does not exist in one dimension. We conjecture that it is a common feature of any dimension  $d \geq 2$ , because the rigid structure necessary to reach a frozen state at density  $\rho = 1/2 - \varepsilon$  results in the quasistationary regime.

Unlike in the one-dimensional case, the diffusion coefficient  $D(\rho)$  has negative exponent (see Table I), and is therefore discontinuous at  $\rho_c$ . We note that the diffusion term operating in the supercritical phase instantly creates at the boundary nonzero density gradients. Therefore, this discontinuity does not create a quantitative different behavior than the  $1d$ -Stefan problem, which has a finite critical diffusion coefficient (12). That is, subcritical regions are frozen while particles in supercritical regions diffuse; and the interfaces between them move as the supercritical regions invade the subcritical ones. The divergence of  $D$  is balanced out by small nonzero density gradients, resulting in a finite current. Hence, as in dimension one, the interfaces move with finite speed.

**Acknowledgments.** This project is partially supported by the ANR grant MICMOV (Grant No. ANR-19-CE40-0012) of the French National Research Agency (ANR). It has received funding from the European Research Council (ERC) under the European Union’s Horizon 2020 research and innovative program (Grant Agreement No. 715734), and from Labex CEMPI (Grant Agreement No. ANR-11-LABX-0007).

A.S., C.E., and M.S. contributed equally to this work; A.R. conducted the numerical simulations.

- [1] S. Torquato, Hyperuniform states of matter, *Phys. Rep.* **745**, 1 (2018).
- [2] P. Bak, *How Nature Works: The Science of Self-Organized Criticality* (Copernicus, New York, NY, 2013).
- [3] R. Dickman, A. Muñoz, A. Vespignani, and S. Zapperi, Paths to self-organized criticality, *Braz. J. Phys.* **30**, 27 (2000).
- [4] P. Bak, C. Tang, and K. Wiesenfeld, Self-organized criticality: An explanation of the  $1/f$  noise, *Phys. Rev. Lett.* **59**, 381 (1987).
- [5] E. Tjhung and L. Berthier, Hyperuniform density fluctuations and diverging dynamic correlations in periodically driven colloidal suspensions, *Phys. Rev. Lett.* **114**, 148301 (2015).
- [6] M. Rossi, R. Pastor-Satorras, and A. Vespignani, Universality class of absorbing phase transitions with a conserved field, *Phys. Rev. Lett.* **85**, 1803 (2000).
- [7] Sometimes, simultaneous jumps are considered [6], but this does not change the critical behavior of the model.
- [8] S. S. Manna, Two-state model of self-organized criticality, *J. Phys. A: Math. Gen.* **24**, L363 (1991).
- [9] R. Dickman, M. Alava, M. A. Muñoz, J. Peltola, A. Vespignani, and S. Zapperi, Critical behavior of a one-dimensional fixed-energy stochastic sandpile, *Phys. Rev. E* **64**, 056104 (2001).
- [10] A. Mukherjee and P. Pradhan, Dynamic correlations in the conserved Manna sandpile, *Phys. Rev. E* **107**, 024109 (2023).
- [11] D. Tapader, P. Pradhan, and D. Dhar, Density relaxation in conserved Manna sandpiles, *Phys. Rev. E* **103**, 032122 (2021).
- [12] D. Hexner and D. Levine, Hyperuniformity of critical absorbing states, *Phys. Rev. Lett.* **114**, 110602 (2015).
- [13] S. Goldstein, J. L. Lebowitz, and E. R. Speer, Approach to hyperuniformity of steady states of facilitated exchange processes, *J. Phys. Condens. Matter.* **36**, 345402 (2024).
- [14] S. Lübeck, Scaling behavior of the absorbing phase transition in a conserved lattice gas around the upper critical dimension, *Phys. Rev. E* **64**, 016123 (2001).
- [15] A. Ayyer, S. Goldstein, J. L. Lebowitz, and E. R. Speer, Stationary states of the one-dimensional facilitated asymmetric exclusion process, *Ann. Inst. H. Poincaré Probab. Statist.* **59**, 726 (2023).
- [16] S. Goldstein, J. L. Lebowitz, and E. R. Speer, Exact solution of the facilitated totally asymmetric simple exclusion process, *J. Stat. Mech.: Theory Exp.* (2019) 123202.
- [17] S. Goldstein, J. L. Lebowitz, and E. R. Speer, The discrete-time facilitated totally asymmetric simple exclusion process, *Pure Appl. Funct. Anal.* **6**, 177 (2021).
- [18] O. Blondel, C. Erignoux, M. Sasada, and M. Simon, Hydrodynamic limit for a facilitated exclusion process, *Ann. Inst. H. Poincaré Probab. Statist.* **56**, 667 (2020).
- [19] O. Blondel, C. Erignoux, and M. Simon, Stefan problem for a nonergodic facilitated exclusion process, *Probability and Mathematical Physics* **2**, 127 (2021).
- [20] C. Erignoux and L. Zhao, Stationary fluctuations for the facilitated exclusion process, [arXiv:2305.13853](https://arxiv.org/abs/2305.13853).
- [21] H. Da Cunha, C. Erignoux, and M. Simon, Hydrodynamic limit for a boundary-driven facilitated exclusion process, [arXiv:2401.16535](https://arxiv.org/abs/2401.16535).
- [22] S. Chatterjee, A. Das, and P. Pradhan, Hydrodynamics, density fluctuations, and universality in conserved stochastic sandpiles, *Phys. Rev. E* **97**, 062142 (2018).
- [23] H. Hinrichsen, Non-equilibrium critical phenomena and phase transitions into absorbing states, *Adv. Phys.* **49**, 815 (2000).
- [24] S. Ghosh and J. L. Lebowitz, Large deviations and rigidity in hyperuniform systems: A brief survey, *Indian J. Pure Appl. Math.* **48**, 609 (2017).
- [25] C. Erignoux, A. Roget, A. Shapira, and M. Simon (unpublished).
- [26] H. Spohn, *Large Scale Dynamics of Interacting Particles* (Springer-Verlag, Berlin, 1991).
- [27] C. Kipnis and C. Landim, *Scaling Limits of Interacting Particle Systems*, Grundlehren der Mathematischen Wissenschaften [Fundamental Principles of Mathematical Sciences] (Springer-Verlag, Berlin, 1999).
- [28] M. Kardar, *Statistical Physics of Particles* (Cambridge University Press, Cambridge, 2007).
- [29] [https://github.com/alexandreroget/2D\\_FacilitatedExclusionProcess](https://github.com/alexandreroget/2D_FacilitatedExclusionProcess).
- [30] C. Arita, P. Krapivsky, and K. Mallick, Bulk diffusion in a kinetically constrained lattice gas, *J. Phys. A: Math. Theor.* **51**, 125002 (2018).
- [31] A. Shapira, Hydrodynamic limit for the Kob–Andersen model, *Ann. Appl. Probab.* **33**, 3493 (2023).
- [32] Y. Zheng, A. D. S. Parmar, and M. Pica Ciamarra, Hidden order beyond hyperuniformity in critical absorbing states, *Phys. Rev. Lett.* **126**, 118003 (2021).